Spatial Correlations in GaInAsN Alloys and their Effects on Band-Gap Enhancement and Electron Localization

Kwiseon Kim and Alex Zunger
National Renewable Energy Laboratory, Golden, Colorado 80401
(Received 14 August 2000)

In contrast to pseudobinary alloys, the relative number of bonds in quaternary alloys cannot be determined uniquely from the composition. Indeed, we do not know if the $Ga_{0.5}In_{0.5}As_{0.5}N_{0.5}$ alloy should be thought of as InAs + GaN or as InN + GaAs. We study the distribution of bonds using Monte Carlo simulation and find that the number of In-N and Ga-As bonds increases relative to random alloys. This quaternary-unique short range order affects the band structure: we calculate a blueshift of the band gap and predict the emergence of a broadband tail of localized states around the conduction band minimum.

DOI: 10.1103/PhysRevLett.86.2609 PACS numbers: 71.20.Nr, 71.55.Eq, 78.20.Bh

The need to simultaneously control both the band gap and the lattice constant of semiconductor alloys prompted interest in not only ternary (e.g., $Ga_{1-x}In_xAs$) but also in quaternary (e.g., $Ga_{1-x}In_xAs_{1-y}P_y$ [1], $Ga_{1-x}In_xAs_{1-y}N_y$ [2]) alloys. The latter class of alloys exhibits a fundamental topological difference with respect to the former class: While in ternary alloys the macroscopic composition x uniquely defines the number of bonds of each type, this is not the case in quaternaries [3]. Indeed, the ratio between the number of In-As and Ga-As bonds in $Ga_{1-x}In_xAs$ is x:$(1-x)$, but in $Ga_{1-x}In_xAs_{1-y}N_y$ the chemical formula itself does not reveal this information, for the number of In-As bonds is not necessarily $x(1-y)M$ nor is the number of Ga-N bonds $(1-x)yM$, where M is the total number of bonds. This means that we do not know if the equimolar system $Ga_{0.5}In_{0.5}As_{0.5}N_{0.5}$ is to be thought of as GaAs + InAs or as GaN + InAs. Since the statistical distribution of bonds of different types controls the optical properties of the alloy (e.g., Ref. [4]), this inherent topological ambiguity in the bond distribution of quaternary alloys poses an important problem.

One can formulate the problem by noting that, in addition to the macroscopic compositions x and y, another parameter ξ must be known in order to specify the nearest-neighbor bond count n_{i-j}. This "short range order" (SRO) parameter can be defined as

$$\xi = n_{\text{In-N}}/M - x_{\text{In}}y_{\text{N}}\,, \tag{1}$$

where $n_{\text{In-As}}/M = x_{\text{In}}(1-y_{\text{N}}) - \xi$, etc. In a perfectly random arrangement, one has $\xi = 0$, whereas $\xi > 0$ means that InN + GaAs is the correct description of the alloy, and $\xi < 0$ means that InAs + GaN is correct. In general, ξ must be determined by minimizing the alloy free energy, yielding the equilibrium function $\xi(x, y, T)$. The following consideration clarifies the main physical factors at play: Since Ga and N are smaller atoms than In and As, respectively, the "small atom–large atom" bond configuration Ga-As + In-N will be better lattice-matched (thus, possess less strain) than the "small atom–small atom" plus "large atom–large atom" bond configuration Ga-N + In-As, respectively. On the other hand, the cohesive energies of the respective binary zinc blende solids follow the sequence [5] GaN > InN > GaAs > InAs (being, respectively, 2.24, 1.93, 1.63, and 1.55 eV per bond), so the (highly strained) Ga-N + In-As configuration is *preferred* in terms of bond energy. Thus, to find the equilibrium configuration, one must search for a configuration that minimizes the sum of strain plus "chemical" (bond) energies, mediated by configurational entropy effects at finite T.

In this Letter we apply finite temperature Monte Carlo (MC) simulation to an empirical energy functional that describes the strain plus chemical energy of GaInAsN for any configuration. We find that (i) $\xi > 0$, so the proper description of this disordered alloy is InN + GaAs. Thus, *N prefers to be surrounded by In atoms ("local In enrichment"), whereas As prefers to be surrounded by Ga.* This type of SRO is a novel feature of quaternary isovalent systems. (ii) This SRO has important consequences on the optical properties of the alloy, leading to significant *blueshift* of the band gap (i.e., reduced bowing) with respect to random alloys. By applying a plane-wave pseudopotential description to large alloy supercells with atomic SRO obtained from the Monte Carlo simulation, we find that the GaInAsN alloy band gap increases by ~100 MeV relative to the random alloy. (iii) The band gap increase is due to the fact that an alloy with SRO has a larger statistical presence of N-centered In_3Ga_1 clusters (local In enrichment), and a smaller presence of N-In_0Ga_4 clusters than in random alloys of the same overall composition. Since the energy level of the N-In_3Ga_1 cluster is higher than that of N-In_0Ga_4 cluster, the statistical depletion of Ga-rich clusters in favor of In-rich clusters leads to a diminished downward level repulsion of the conduction band, relative to the random alloy, hence to a larger band gap. This discovery of SRO-induced band-gap shift is important since one might hope to control $\xi(x, y, T)$, and thus the band gap, via control of growth conditions. (iv) While it was previously

thought (e.g., Ref. [1]) that, in quaternary semiconductor alloys, one can simultaneously tune band gaps and the lattice constant by altering only the composition (x, y), we find that the ensuing band gap is, in fact, not unique and an additional thermodynamic variable (ξ_{SRO}) controls it. (v) The level repulsion in the conduction band has an important consequence on localization: While the statistical distribution of As-centered As-Ga_mIn_{4-m} tetrahedra in ternary InGaAs causes a small ($\sim$1 meV) broadening of the conduction band minimum (CBM), the distribution of N-centered N-Ga_mIn_{4-m} tetrahedra in GaInAsN leads to a far broader range ($\sim$60 meV) of quasi-N-localized band tail states near the CBM. This wide range is due to the stronger perturbations by the higher energy cluster (L_{1c}-derived) levels in the nitride alloy. Such strong alloy band edge fluctuations can locally capture carriers, affecting carrier dynamics [6].

Our model energy functional depends both on site occupancy variables S_c, S_a and on atomic positions $\mathbf{R}_i$:

$$E[\{S_c; S_a\}; \{\mathbf{R}_i, i = 1, \ldots, M\}] = E_{\mathrm{chem}} + E_{\mathrm{strain}} . \quad (2)$$

Here $S_c = 1$ (-1) if Ga (In) is on cation site c, and $S_a = 1$ (-1) if As (N) is on the anion site a. Also, $\{\mathbf{R}_i, i = 1, \ldots, M\}$ are the atomic positions of all M atoms in the cell. Since we are not aiming at an accurate calculation of the absolute energy E but rather the atomic configuration $\{S_c; S_a\}$ that has the best balance of strain vs bond energy, a simple energy functional is sufficient. We use

$$E_{\mathrm{chem}} = \frac{1}{2} \sum_i \sum_j^{nn} n_{i-j} e_{ij} , \quad (3)$$

where n_{i-j} is the number of bonds of type ij, and e_{ij} is the respective bond energy for which we use the experimental cohesive energy [5] of binary compound ij. For a ternary such as $Ga_{1-x}In_xAs$, the chemical energy E_{chem} is a configuration independent constant $xE_{\mathrm{InAs}} + (1 - x)E_{\mathrm{GaAs}}$ and hence does not decide the thermodynamic energy balance. This is so because, in a ternary, any cation (Ga or In) atom is always bonded to As atoms, regardless of the configuration. For the strain energy we use the valence force field (VFF) model [7] and bond-stretching and bond-bending force constants of Refs. [8,9].

We start with the simplest case of $T = 0$. The energies of some limiting thermodynamic states, e.g., the random alloy or phase separation into constituents that are *coherent* with the substrate, are depicted in the upper half of Fig. 1(a). We consider an alloy that is lattice-matched to a given substrate. This produces a relationship between x_{In} and y_{N} for each substrate. The energy of the random $\xi = 0$ alloy is calculated in Fig. 1(a) by relaxing atomic positions of the random configuration using the VFF method while maintaining coherence. Figure 1(a) shows that for a GaAs substrate, at $T = 0$, phase separation into the strain-minimizing (but chemically unfavorable) InN + GaAs configuration is much lower in energy than phase separation into the chemical-energy-minimizing (but highly strained) InAs + GaN configuration. If one removes the coherence condition, permitting each material to attain its own lattice parameter [so that $E_{\mathrm{strain}} = 0$, see bottom half of Fig. 1(a)], then InAs + GaN is the preferred decomposition. Note that, near the free surface, atoms can relax freely so that $E_{\mathrm{strain}} \approx 0$ and the preferred configuration is GaN + InAs, just as in the incoherent case.

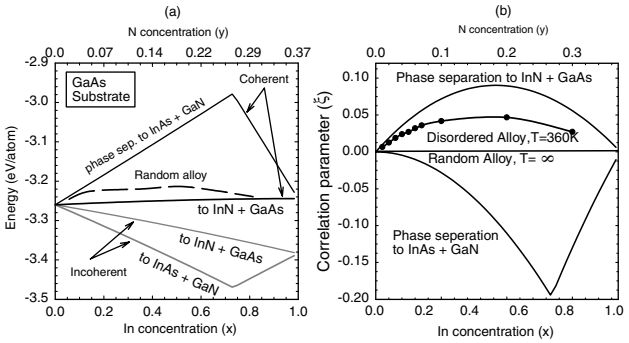

FIG. 1. (a) The energies of some limiting thermodynamic states of GaInAsN lattice-matched to GaAs at $T = 0$. The lowest energy for *coherent* phase separation (upper part) is for InN + GaAs while, for *incoherent* phase separation (lower part), the lowest energy is for InAs + GaN. (b) The SRO parameter ξ [Eq. (1)] expected for the limiting cases of phase separation into InN + GaAs and InAs + GaN lattice-matched to GaAs. For the random alloy, $\xi = 0$, whereas for the disordered alloy with SRO at $T = 360$ K, $\xi > 0$.

Figure 1(b) shows the ξ expected for the limiting cases of phase separation at $T = 0$ for the $Ga_{1-x}In_xAs_{1-y}N_y$ lattice-matched to GaAs. For phase separation into InN + GaAs, the proportion of InN bonds is the lesser of x and y (in this case, y), thus $\xi = y - xy \approx (1 - 2.7y)y$, which is positive. For the InAs + GaN case, there are two cases: (i) when $y < 1 - x$, the number of InN bonds is 0, thus $\xi = -xy \approx -2.7y^2$, which is negative. (ii), when $y > 1 - x$, the proportion of InN bonds is $x + y - 1$, thus $\xi = -(1 - x)(1 - y) \approx -(1 - 2.7y)(1 - y)$, which is also negative.

The next question is how these $T = 0$ behaviors of Figs. 1(a) and 1(b) are modified at finite temperatures. To obtain finite-temperature results we subject our energy functional of Eq. (2) to a MC treatment, randomly flipping spins and simultaneously relaxing atomic positions, so as to minimize the energy of each spin configuration. This "spin flip + atomic relaxation MC" [10] is executed using a cell of 512 atoms with 100 000 spin flips per temperature (clearly, a first-principles energy functional for Eq. (2) is prohibitively costly). The simulation temperature is exponentially lowered with 12 steps, to equilibrate the configuration at each temperature as it reaches the ground state at the low temperature. Figure 1(b) shows the resulting $\xi(x, y, T)$ at $T = 360$ K. Our result shows that, for GaInAsN, $\xi > 0$, i.e., the InN + GaAs configuration is preferred. The SRO parameter ξ is *positive*, being about 0.013 and 0.004 for $Ga_{0.94}In_{0.06}As_{0.98}N_{0.02}$ at 360 and 1200 K, respectively, and 0.042 and 0.031 for $Ga_{0.75}In_{0.25}As_{0.91}N_{0.09}$ at 360 and 1200 K, respectively.

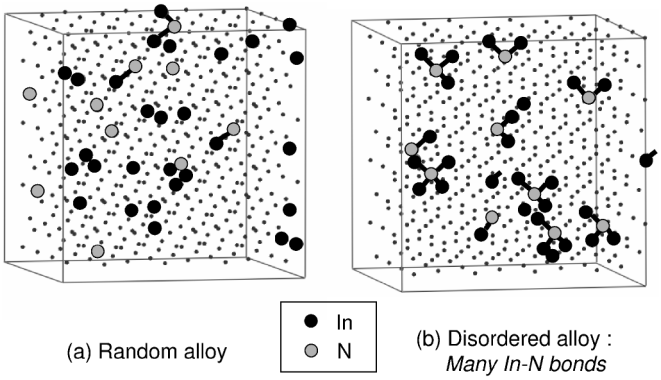

FIG. 2. A visualization of the real space supercell of the alloy $Ga_{0.89}In_{0.11}As_{0.96}N_{0.04}$ (a) for a random configuration and (b) with SRO determined by MC simulation at $T = 360$ K. Note the preponderance of N-In_3Ga_1 and N-In_4 clusters. Solid dots denote the positions of Ga and As atoms.

Figure 2 provides a visualization of the real space atomic positions in the supercell of $Ga_{0.89}In_{0.11}As_{0.96}N_{0.04}$ with SRO obtained with MC simulation at $T = 360$ K. Taking statistics over many final configurations such as that shown in Fig. 2 reveals that *the main effect of SRO is that the concentration of the N-centered In_3Ga_1 clusters is statistically enhanced significantly (local In enrichment), whereas the In_0Ga_4 clusters are statistically depleted relative to the random alloy.* Also, the first nearest-neighbor N-N pairs are depleted and the third nearest-neighbor N-N pairs ("NN3") are enhanced.

To understand the consequence of this special quaternary SRO on the *electronic* properties, we calculated the energy levels of supercells such as Fig. 2 by using the empirical pseudopotential method (EPM) as described in Ref. [11]. We use the pseudopotential parameters of Bellaiche [12]. Comparing the band gap of a $Ga_{0.94}In_{0.06}As_{0.98}N_{0.02}$ supercell with MC-determined SRO to that of an equivalent random alloy, we see that SRO *increases* the band gap by $\sim$100 meV, thus reducing the optical bowing. This effect is similar to the case of $Zn_{1-x}Mg_xS_{1-y}Se_y$ alloys, where clustering of MgS + ZnSe also increases the band gap [13], but the effect here is considerably larger. Figure 3 depicts the most important energy levels calculated for (i) isolated N in GaAs, (ii) *isolated* N-In_mGa_{4-m} clusters ($0 \le m \le 4$), each embedded in the *ternary* $In_{0.06}Ga_{0.94}As$, (iii) *concentrated* (rather than isolated) but *random* 2% N alloy of $Ga_{0.94}In_{0.06}As_{0.98}N_{0.02}$, and (iv) correlated (rather than random) 2% N alloy of $Ga_{0.94}In_{0.06}As_{0.98}N_{0.02}$. To identify the nature of the levels we project the corresponding alloy wave functions onto the Γ, L, and X Bloch wave functions [14], and indicate in Fig. 3 the percentage character. We note the following features.

(i) *Isolated N-In_pGa_{4-p} clusters in InGaAs.*—Much like an *isolated* N impurity in GaAs [Fig. 3(a)] introduces an a_1(N) N-localized level above the CBM (at $E_c + 180$ meV) and an L_{1c}-derived level $a_1(L_{1c})$ at [14] $E_c + 286$ meV, so does *isolated* N in GaInAs [Fig. 3(b)].

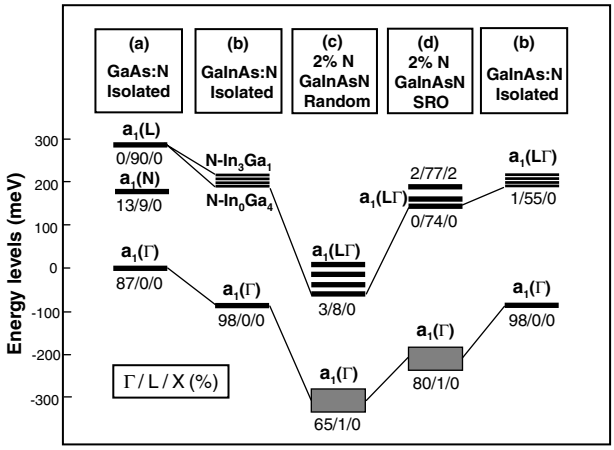

FIG. 3. The most important energy levels with $(\Gamma/L/X)$ percentages calculated for (a) isolated N in GaAs, (b) isolated N-In_mGa_{4-m} clusters ($0 \le m \le 4$) each embedded in a 4096-atom supercell of $In_{0.06}Ga_{0.94}As$, (c) *random* 2% N alloy of $Ga_{0.94}In_{0.06}As_{0.98}N_{0.02}$, and (d) SRO 2% N alloy of $Ga_{0.94}In_{0.06}As_{0.98}N_{0.02}$. Shaded areas denote band tails. The zero of energy is the CBM of GaAs.

However, here one can distinguish five different types of isolated nitrogens, depending on their nearest-neighbor coordination N-In_mGa_{4-m}, where $0 \le m \le 4$. We can determine the energies of such clusters in the ultradilute limit by placing them, one at a time, in a large GaInAs supercell [Fig. 3(b)]. We find that the energy of the N-centered In_0Ga_4 level is the lowest, occurring at $E_c + 215$ meV, while the In_3Ga_1 level is highest, occurring at $E_c + 229$ meV, where E_c is the CBM energy of GaAs. The N-cluster levels are strongly localized around N and their wave functions are composed mainly of the L_{1c} alloy states. The alloy CBM at $E_c - 90$ meV is a delocalized Γ_{1c}-like state. Note in Fig. 3 that the N level in GaAs:N is closer to the CBM of GaAs than the N levels in InGaAs:N. Thus, the addition of N to InGaAs causes weaker coupling to the CBM (less bowing) than the addition of N to GaAs. Specifically, 1% N reduces the GaAs gap by 90 meV more than it reduces the InGaAs gap. We will next see that SRO in GaInAsN further reduces the bowing relative to *random* GaInAsN.

(ii) *Concentrated N-In_pGa_{4-p} clusters in InGaAs alloy.*—As the N concentration increases from the ultradilute limit [Fig. 3(b)] to 2% [Fig. 3(c)], all conduction levels move down in energy, reflecting the alloy's large bowing parameter [15]. Since we have only 6% In in our alloy, in a *random arrangement* the In-poor clusters In_0Ga_4 and In_1Ga_3 form statistically the majority clusters. But, in a *correlated arrangement,* with SRO [Fig. 3(d)] the In-poor In_0Ga_4 and In_1Ga_3 clusters are statistically nearly eliminated in favor of In-rich In_3Ga_1 clusters, (See also Fig. 2) even though the total In content is conserved. Since the L_{1c}-like energy level of the In_0Ga_4 cluster is closer to the alloy Γ_{1c}-like CBM [Fig. 3(b)], the L_{1c}-like level would interact more strongly with the Γ_{1c}-like CBM than with the higher energy level of the In_3Ga_1 cluster. Consequently,

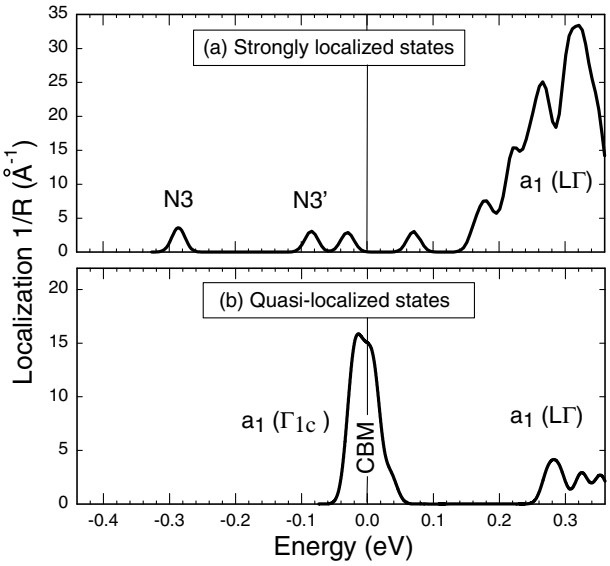

FIG. 4. Average of inverse of the localization radius $R(\epsilon_i)$ (the radius around N that contains 20% of the amplitude of the wave function) vs the energy ϵ_i. (a) The distribution of localized states for which there are at least 10% of N with the value of $R < 13$ Å. (b) The distribution of the rest less-localized states. The zero of energy is the average alloy CBM.

in the *random alloy* with its statistically abundant In_0Ga_4 clusters, the alloy CBM is pushed downwards more ($\sim$200 meV) than in the SRO alloy, which lacks In_0Ga_4 clusters. This explains why the correlated alloy has a larger band gap (smaller bowing) than the random alloy.

(iii) *Localized states near the CBM.*—The mechanism of the repulsion between the L_{1c}-like N-In_mGa_{4-m} cluster states and the Γ_{1c}-like CBM leads to another interesting effect—strong alloy potential fluctuations near the CBM. Because the N-In_mGa_{4-m} clusters have an inherent statistical distribution of m values (unlike N in *pure* GaAs, having a single N-Ga_4 local nearest-neighbor environment), and because the energies of these L_{1c}-like cluster levels depend strongly on m (shifting by 14 meV for $m = 1$ to $m = 3$, far more than the 0.1 meV shift in As-centered clusters), we find a corresponding *broad distribution* of Γ_{1c}-like band tail levels near the CBM. By distributing 2% N (41 atoms) in a 4096-atom cell of $In_{0.06}Ga_{0.94}As$ in 15 independent configurations σ and calculating the electronic structure, we are able to examine the *distribution* of localized states near the CBM. To see the localization, we calculate for each N site α in alloy configuration σ the radius $R_\alpha(\sigma, \epsilon)$ that localizes within it 20% of the wave function $\psi(\epsilon)$ at energy ϵ. Figure 4(a) shows the distribution of strongly localized states, while Fig. 4(b) shows the distribution of the rest, less-localized states. We see in Fig. 4(b) a $\sim$60 meV (FWHM) wide distribution of Γ_{1c}-like band tail states (compared with $\sim$1 meV in InGaAs). The Γ_{1c} broadening results from different degrees of repulsion of Γ_{1c} by the higher energy N-In_mGa_{4-m} cluster states of L_{1c} character [16]. Below the $a_1(\Gamma_{1c})$ CBM we see strongly localized states inside the gap: the nearest-neighbor pairs N-N and triplets N3 and N3′. These gap states and the quasilocal Γ_{1c}-like band tail states could explain the very different carrier dynamics in quaternary GaInAsN relative to the ternary InGaAs (Ref. [6]) including the longer lifetime associated with stronger alloy fluctuations (e.g., Ref. [18]) and weaker temperature dependence of the band gap (Ref. [19]).

In summary, we find that the strong perturbation of the N-centered clusters leads in the quaternary GaInAsN to a special form of SRO, a blueshift of the gap, reduced bowing, and broad, localized band tail states as well as band-gap levels.

This work was supported by the DOE/OS/BES/MSD under Contract No. DE-AC36-99-GO10337. We thank L. Bellaiche for providing us with his EPM parameters.

[1] *GaInAsP Alloy Semiconductors,* edited by T. P. Pearsall (Wiley, New York, 1982).
[2] M. Kondow *et al.,* IEEE J. Quantum Electron. **3**, 719 (1997).
[3] M. Ichimura and A. Sasaki, Phys. Rev. B **36**, 9694 (1987).
[4] R. Magri and A. Zunger, Phys. Rev. B **44**, 8672 (1991).
[5] W. A. Harrison, *Electronic Structure and the Properties of Solids* (Dover, New York, 1989), p. 176.
[6] H. Mariette, Physica (Amsterdam) **146B**, 286 (1987); H. Mariette, Solid State Commun. **38**, 1193 (1981).
[7] P. N. Keating, Phys. Rev. **145**, 637 (1966); R. M. Martin, Phys. Rev. B **1**, 4005 (1970).
[8] J. Martins and A. Zunger, Phys. Rev. B **30**, 6217 (1984).
[9] K. Kim *et al.,* Phys. Rev. B **53**, 16 310 (1996).
[10] A. Silverman *et al.,* Phys. Rev. B **51**, 10 795 (1995).
[11] T. Mattila *et al.,* Phys. Rev. B **59**, 15 270 (1999).
[12] L. Bellaiche, Appl. Phys. Lett. **75**, 2578 (1999).To circumvent the need for "charge self-consistency," this potential depends explicitly on the chemical environment of an atom (e.g., Ga surrounded by different numbers of N and As atoms) and was fitted explicitly to band gaps and effective masses of the binary compounds and to the optical bowing of ternary alloys.
[13] A. M. Saitta *et al.,* Appl. Phys. Lett. **75**, 2746 (1999); *ibid.,* Phys. Rev. Lett. **80**, 4939 (1998).
[14] T. Mattila *et al.,* Phys. Rev. B **60**, R11 245 (1999).
[15] S.-H. Wei and A. Zunger, Phys. Rev. Lett. **76**, 664 (1996).
[16] In the simplified model of Shan *et al.* (Ref. [17]), the repulsion is instead between the CBM and a_1(N). Also, their model neglects alloy fluctuations so the band edge states are sharp.
[17] W. Shan *et al.,* Phys. Rev. Lett. **82**, 1221 (1999).
[18] R. K. Ahrenkiel *et al.* Appl. Phys. Lett. (to be published).
[19] A. Polimeni *et al.,* Appl. Phys. Lett. **77**, 2870 (2000).